

## Direct Antiviral Activity of IFN-Stimulated Genes Is Responsible for Resistance to Paramyxoviruses in ISG15-Deficient Cells

This information is current as of May 29, 2020.

David Holthaus, Andri Vasou, Connor G. G. Bamford, Jelena Andrejeva, Christina Paulus, Richard E. Randall, John McLauchlan and David J. Hughes

*J Immunol* published online 18 May 2020  
<http://www.jimmunol.org/content/early/2020/05/15/jimmunol.1901472>

**Supplementary Material** <http://www.jimmunol.org/content/suppl/2020/05/15/jimmunol.1901472.DCSupplemental>

Why *The JI*? [Submit online.](#)

- **Rapid Reviews! 30 days\*** from submission to initial decision
- **No Triage!** Every submission reviewed by practicing scientists
- **Fast Publication!** 4 weeks from acceptance to publication

*\*average*

**Subscription** Information about subscribing to *The Journal of Immunology* is online at: <http://jimmunol.org/subscription>

**Permissions** Submit copyright permission requests at: <http://www.aai.org/About/Publications/JI/copyright.html>

**Author Choice** Freely available online through *The Journal of Immunology* [Author Choice option](#)

**Email Alerts** Receive free email-alerts when new articles cite this article. Sign up at: <http://jimmunol.org/alerts>

*The Journal of Immunology* is published twice each month by The American Association of Immunologists, Inc., 1451 Rockville Pike, Suite 650, Rockville, MD 20852  
Copyright © 2020 The Authors All rights reserved.  
Print ISSN: 0022-1767 Online ISSN: 1550-6606.



# Direct Antiviral Activity of IFN-Stimulated Genes Is Responsible for Resistance to Paramyxoviruses in ISG15-Deficient Cells

David Holthaus,<sup>\*,1,2</sup> Andri Vasou,<sup>\*,1</sup> Connor G. G. Bamford,<sup>†,3</sup> Jelena Andrejeva,<sup>\*</sup> Christina Paulus,<sup>\*</sup> Richard E. Randall,<sup>\*</sup> John McLauchlan,<sup>†</sup> and David J. Hughes<sup>\*</sup>

IFNs, produced during viral infections, induce the expression of hundreds of IFN-stimulated genes (ISGs). Some ISGs have specific antiviral activity, whereas others regulate the cellular response. Besides functioning as an antiviral effector, ISG15 is a negative regulator of IFN signaling, and inherited ISG15 deficiency leads to autoinflammatory IFNopathies, in which individuals exhibit elevated ISG expression in the absence of pathogenic infection. We have recapitulated these effects in cultured human A549-ISG15<sup>-/-</sup> cells and (using A549-UBA7<sup>-/-</sup> cells) confirmed that posttranslational modification by ISG15 (ISGylation) is not required for regulation of the type I IFN response. ISG15-deficient cells pretreated with IFN- $\alpha$  were resistant to paramyxovirus infection. We also showed that IFN- $\alpha$  treatment of ISG15-deficient cells led to significant inhibition of global protein synthesis, leading us to ask whether resistance was due to the direct antiviral activity of ISGs or whether cells were nonpermissive because of translation defects. We took advantage of the knowledge that IFN-induced protein with tetratricopeptide repeats 1 (IFIT1) is the principal antiviral ISG for parainfluenza virus 5. Knockdown of IFIT1 restored parainfluenza virus 5 infection in IFN- $\alpha$ -pretreated, ISG15-deficient cells, confirming that resistance was due to the direct antiviral activity of the IFN response. However, resistance could be induced if cells were pretreated with IFN- $\alpha$  for longer times, presumably because of inhibition of protein synthesis. These data show that the cause of virus resistance is 2-fold; ISG15 deficiency leads to the early overexpression of specific antiviral ISGs, but the later response is dominated by an unanticipated, ISG15-dependent loss of translational control. *The Journal of Immunology*, 2020, 205: 000–000.

**T**he innate immune response against pathogens is underpinned by the evolutionary conserved IFN system. All cells express pathogen recognition receptors (PRRs) that sense the products of infection and establish a signaling cascade leading to the production of cytokines, including type I IFN (IFN- $\alpha$ / $\beta$ )

(1, 2). IFN is secreted from cells and binds to cell surface receptors expressed on both infected and noninfected cells, initiating a JAK/STAT signaling cascade, culminating in the expression of hundreds of IFN-stimulated genes (ISGs) (3). The biological effects of ISGs are extensive, and their principle role is to generate an unfavorable environment for the replication of viruses. Many ISGs have broad antiviral activity, such as dsRNA-dependent protein kinase R (PKR) that, upon recognition of viral dsRNA, dampens general protein synthesis and prevents the translation of viral mRNAs (4). Other antiviral ISGs, such as IFN-induced protein with tetratricopeptide repeats (IFIT) proteins, inhibit specific viruses, but for many, they are inconsequential (5). Additionally, multiple ISGs are generally required to limit infection because the majority of ISGs result in low to moderate levels of inhibition (6); however, ISGs with specific antiviral properties for a given virus are often not known. Nevertheless, the nature of the innate immune response necessitates the production of the complete spectrum of ISGs, albeit with a high degree of redundancy, as during a natural infection, the identity of the infecting virus is not known. This response is inevitably tightly regulated, as a dysregulated response leads to a suite of autoinflammatory diseases (7).

The ubiquitin-like protein (Ubl) ISG15 is strongly induced by IFN and is critical for regulating how cells respond to infection. As a posttranslational modification, it can covalently modify proteins in a process known as ISGylation, and in many cases, modification of viral proteins forms part of the antiviral response (8). Covalently bound ISG15 can also be removed from proteins by the ubiquitin-specific protease 18 (USP18) (9). Importantly, loss-of-function mutations in ISG15 have been identified in human patients with subsets of autoinflammatory IFNopathies, and typically, these individuals demonstrate elevated ISG expression in the absence of pathogenic infection (10). Mechanistically, it was shown that ISG15

\*Biomedical Sciences Research Complex, School of Biology, University of St Andrews, St Andrews KY16 9ST, United Kingdom; and <sup>†</sup>MRC-University of Glasgow Centre for Virus Research, Glasgow G61 1QH, United Kingdom

<sup>1</sup>D.H. and A.V. contributed equally.

<sup>2</sup>Current address: Unit 16 Mycotic and Parasitic Agents and Mycobacteria, Robert Koch-Institute, Berlin, Germany.

<sup>3</sup>Current address: Wellcome-Wolfson Institute for Experimental Medicine, Queen's University, Belfast, U.K.

ORCID: 0000-0002-7012-5605 (D.H.); 0000-0002-4123-5629 (C.P.); 0000-0002-9304-6678 (R.E.R.); 0000-0003-2217-9948 (J.M.); 0000-0002-0090-5710 (D.J.H.).

Received for publication December 12, 2019. Accepted for publication April 23, 2020.

This work was supported by Academy of Medical Sciences Grant SBF003/1028, Wellcome Trust Grant 101788/Z/13/Z, U.K. Research and Innovation, Medical Research Council Grant MC\_UU\_12014/1, and Erasmus+ (to D.H.).

Address correspondence and reprint requests to Dr. David J. Hughes, Willie Russell Laboratories, University of St Andrews, North Haugh, St Andrews, KY16 9ST Fife, U.K. E-mail address: djh25@st-andrews.ac.uk

The online version of this article contains supplemental material.

Abbreviations used in this article: CEACAM1, carcinoembryonic Ag-related cell adhesion molecule 1; Ct, cycle threshold; HPIV2, human parainfluenza virus 2; IFIT, IFN-induced protein with tetratricopeptide repeat; ISG, IFN-stimulated gene; Met, methionine; MOI, multiplicity of infection; NP, nucleoprotein; N-pro, N-terminal protease; P, phosphoprotein; p.i., postinfection; PIV5, parainfluenza virus 5; PIV5-CPI<sup>-</sup>, PIV5 strain CPI<sup>-</sup>; PIV5-W3, PIV5 strain W3; PKR, protein kinase R; sgRNA, single-guide RNA; shIFIT1, short hairpin IFIT1; USP18, ubiquitin-specific protease 18.

This article is distributed under the terms of the [CC BY 4.0 Unported license](https://creativecommons.org/licenses/by/4.0/).

Copyright © 2020 The Authors

functions as a negative regulator of type I IFN signaling by stabilizing USP18, a known inhibitor of JAK/STAT signaling (11–13). Intriguingly, despite the known functions of ISG15 and USP18 in the ISGylation process, the regulation of type I IFN signaling was entirely independent of ISGylation (10). Interestingly, mouse *Isg15* is not required to stabilize *Usp18* and appears not to be needed to regulate IFN signaling, suggesting a species-specific gain of function for human ISG15 (14).

Previous work has shown that cells from ISG15-deficient patients expressed higher levels of ISGs compared with normal controls when treated with rIFN- $\alpha$ , and these cells were resistant to several viruses (14); however, it was not clear at what stage of infection viruses were blocked or how. Furthermore, cells were treated with IFN- $\alpha$ , followed by washing (to remove IFN), and rested for 36 h prior to infection. Because ISG15 is involved in regulating the cell cycle (15) and protein synthesis (shown in this report), an overamplified IFN response (because of lack of ISG15 and reduced levels of USP18) may have led to virus resistance simply because cells were no longer permissive to infection. This has implications for our understanding as to why ISG15-deficient patients are not more susceptible to viral infections; these observations have led to the suggestion that, unlike in mice, human ISG15 is not an antiviral effector (14, 16).

In this study, we recapitulated the phenotype observed in ISG15-deficient patient cells upon treatment with rIFN- $\alpha$  in a cell culture model and dissected the mechanisms that result in virus resistance during an antiviral state. We showed that resistance was due to the direct antiviral activity of the type I IFN response and discuss the implications of ISG15 loss of function during the innate immune response. Based on our findings, we conclude that observations from ISG15-deficient patients alone cannot be used to infer that ISG15 does not possess antiviral effector functions, as has been proposed (14, 16).

## Materials and Methods

### Cells

Vero cells (African green monkey kidney epithelial cells), A549 cells (human adenocarcinoma alveolar basal epithelial cells), and derivatives were maintained in DMEM (Sigma-Aldrich) supplemented with 10% (v/v) heat-inactivated FBS (Biowest) and incubated in 5% (v/v) CO<sub>2</sub> at 37°C in a humidified incubator. A549–short hairpin IFIT1 (shIFIT1) have been described elsewhere (17) and were maintained in blasticidin (10  $\mu$ g/ml). A549-*ISG15*<sup>-/-</sup> cells were generated by CRISPR/Cas9n system that uses the D10A dual “nickase” mutant of Cas9 (Cas9n) that ostensibly limits off-target effects. Briefly, to disrupt exon 2 of the *ISG15* gene, single-guide RNA (sgRNA) sequences were cloned using pPX460 and transfected into A549 cells as previously described (18). Transfectants were enriched by treating cells with puromycin (1  $\mu$ g/ml) for 2 d and then diluted to single cells in 96-well plates. Correctly edited cell clones were verified by immunoblot analysis. A549-*ISG15*<sup>-/-</sup>-shIFIT1 cells were generated as previously described using A549-*ISG15*<sup>-/-</sup> (B8) and maintained in media with blasticidin (10  $\mu$ g/ml) (17). To generate A549-*UBA7*<sup>-/-</sup> cells, A549 cells were first made to stably express *Streptococcus pyogenes* Cas9 following blasticidin selection of cells transduced with lentiCas9-Blast [gift from F. Zhang, plasmid no. 52962; Addgene (19)]. The sgRNA sequence that targeted exon 3 of *UBA7* was chosen computationally (<https://www.deskgen.com>), and complementary oligonucleotides (sense: 5'-caccGCACACGGGTGACATC-*ACTG*-3'; antisense: 5'-aaacCAGTGATGTCACCCGTGTGC-3') were hybridized and ligated into the *Bsm*BI site of pLentiGuide-Puro [gift from F. Zhang, no. 52963; Addgene (20)]. Cas9-expressing A549s were transduced with *UBA7* sgRNA-expressing lentiGuide-Puro and selected with puromycin. Puromycin-resistant cells were single-cell cloned by FACS, and successful knockout cells were validated by immunoblot analysis. A549 cells expressing the N-terminal protease (Npro) from bovine viral diarrhea virus (BVDV), namely A549-Npro cells, have been described previously (21).

### Virus infections and treatments

Viruses used were human parainfluenza virus 2 (HPIV2) strain Colindale, HPIV3 strain Washington/47885/57 (20), parainfluenza virus 5 (PIV5)

strain W3 (22), and PIV5 strain CPI<sup>-</sup> (PIV5-CPI<sup>-</sup>) (23). Virus stocks were prepared by inoculating Vero cells at a multiplicity of infection (MOI) of 0.001 with continual rocking at 37°C. Supernatants were harvested at 2 d postinfection (p.i.), clarified by centrifugation at 3000  $\times$  g for 15 min, aliquoted, and snap frozen. Titers were estimated by standard plaque assay on Vero cells in six-well plates.

For infection studies, cell monolayers were infected in six-well plates with virus diluted in medium to achieve an MOI of 10, unless stated otherwise. Virus adsorption was for 1 h, after which the viral inoculum was removed and replaced with media supplemented with 2% (v/v) FBS and incubated in 5% (v/v) CO<sub>2</sub> at 37°C until harvested. When cells were treated with IFN- $\alpha$  prior to infection (pretreated), this was done with 1000 IU/ml IFN- $\alpha$ 2b (referred to as IFN- $\alpha$  in this article; IntronA; Merck Sharp & Dohme) 18 h prior to infection, unless otherwise stated. IFN- $\alpha$  remained on cells for the duration of experiments. Cells were either processed for immunoblot analysis or (if infecting with rPIV5-mCherry, kind gift from Dr. He, University of Georgia) imaged using an InCuCyte ZOOM imaging system (Sartorius).

For plaque assays 30–40 PFU PIV5-CPI<sup>-</sup> in 1 ml DMEM, 2% FBS was adsorbed for 1 h onto confluent monolayers of cells in six-well plates while rocking at 37°C. Following adsorption, 2 ml overlay (DMEM and 2% FBS; Avicel) was added to wells and incubated for 6 d. Cells were fixed with 5% formaldehyde (10 min), washed in PBS, and either stained for 10 min with 1 mg/ml Toluidine Blue O (Sigma-Aldrich), followed by rinses with water, or permeabilized for 10 min (PBS, 1% Triton X-100, and 3% FBS), washed again, and incubated for 1 h with a pool of PIV5-specific Abs (24) or mouse monoclonal anti-HPIV3 nucleoprotein (NP) (25) diluted in PBS and 3% FBS (1:1000). Following PBS washes, cells were incubated for 1 h with goat anti-mouse IgG Abs conjugated to alkaline phosphatase (catalog no. ab97020; Abcam) diluted 1:1000 in PBS and 3% FBS. Cells were washed in PBS, and signals were detected using SIGMAFAST BCIP/NBT (Sigma-Aldrich).

### Reverse transcription quantitative PCR

To quantify ISG expression, total cellular RNA was purified from cells that had been treated with 1000 IU/ml IFN- $\alpha$  for 18 h or left untreated using TRIzol reagent (Thermo Fisher Scientific) and Direct-zol RNA Miniprep Plus Kits, followed by on-column DNase I treatment for the removal of contaminating DNA (Zymo Research). To measure PIV5 strain W3 (PIV5-W3) transcription, the indicated cells were treated with 1000 IU/ml IFN- $\alpha$ 2b for 8 h and then infected with PIV5 (MOI 10). Following adsorption for 1 h at 37°C, cells were lysed in TRIzol at the indicated times, and RNA was purified as above. cDNA was synthesized in 20  $\mu$ l reaction volumes with 500 ng (ISGs) or 100 ng (PIV5-infected cells) total RNA and oligo(dT) using GoScript reverse transcriptase (Promega) according to the manufacturer's recommendations. Quantitative PCR mixes (20  $\mu$ l) included 1 $\times$  PerfeCTa SYBR Green SuperMix (Quanta BioSciences), 0.5  $\mu$ M each primer, and 1  $\mu$ l cDNA reaction mixture. Cycling was performed in an Mx3005P real time PCR machine (StrataGene) and included an initial 3-min enzyme activation step at 95°C, followed by 40 cycles of 10 s at 95°C, 10 s at 58°C, and 20 s at 72°C. Melting curve analysis was performed to verify amplicon specificity. Quantification of  $\beta$ -*ACTIN* mRNA was used to normalize between samples, and the average cycle threshold (Ct) was determined from three independent cDNA samples from independent cultures. Relative expression compared with nontreated control cells was calculated using the  $\Delta\Delta$ Ct method. Primer sequences were the following: *HERC5* 5'-GACGAACCTTGTGACCGTCTC-3' and 5'-GCGTCCACAGTCATTTC-CAC-3', *USP18* 5'-ATGCTGCCCACTGTACCTC-3' and 5'-CCTGCA-GTCTCTCCACCAAG-3', *MxA* 5'-GCCTGTGACATTGGGTATAA-3' and 5'-CCCTGAAATATGGGTGGTCTC-3', *IFIT1* 5'-CCTGGAGTAC-TATGAGCGGGC-3' and 5'-TGGGTGCCTAAGGACCTTGTC-3', *PIV5 NP* 5'-AGGGTAGAGATCGATGGCT-3' and 5'-GTCTGACCACCATC-CCCT-3', and  $\beta$ -*ACTIN* 5'-AGCGAGCATCCCCAAAGTT-3' and 5'-AGGGCACGAAGGCTCATCATT-3'.

### Immunoblotting

Confluent monolayers in six-well dishes were lysed with 250  $\mu$ l 2 $\times$  Laemmli sample buffer (4% w/v SDS, 20% v/v glycerol, 0.004% w/v bromophenol blue, and 0.125 M Tris-HCl (pH 6.8) with 10% v/v 2-ME) for 10 min, incubated at 95°C for 10 min, sonicated at 4°C with three cycles of 30 s on/30 s off in a Bioruptor Pico (Diagenode) and clarified by centrifugation at 12,000  $\times$  g, 4°C for 10 min. SDS-PAGE in Tris-glycine-SDS running buffer and immunoblotting followed standard techniques using the following Abs: mouse monoclonal anti-ISG15 F-9 (catalog no. sc166755; Santa Cruz Biotechnology), rabbit polyclonal anti-MxA (catalog no. 13750-1-AP; Proteintech), goat polyclonal anti-IFIT1 N-16 (catalog no. sc82946; Santa Cruz Biotechnology), mouse monoclonal anti- $\beta$ -*ACTIN*,

UBA7 (anti-UBE1L B-7; catalog no. sc-390097; Santa Cruz Biotechnology), rabbit monoclonal anti-phosphorylated STAT1 (anti-phospho-STAT1 [Tyr<sup>701</sup>] 58D6; catalog no. 9167; Cell Signaling Technology), mouse monoclonal anti-PIV5 NP 125 (24), mouse monoclonal anti-HPIV2 and anti-PIV5 phosphoprotein (P) 161 [Ab cross-reacts with P of both viruses (24)], and mouse monoclonal anti-HPIV3 NP (25). For quantitative immunoblots, primary Ab-probed membranes were incubated with IRDye Secondary Abs (LI-COR Biosciences) and signals detected using an Odyssey CLX scanner. Data were processed and analyzed using Image Studio software (LI-COR Biosciences).

### <sup>35</sup>S-methionine labeling

Subconfluent A549 and A549-*ISG15*<sup>-/-</sup> (B8) cells in six-well plates were treated with 1000 IU/ml IFN- $\alpha$  or left untreated. At 24, 48, and 72 h following treatment, cells were pulse labeled with 500 Ci/mmol <sup>35</sup>S-methionine (Met; MP Biomedical) in Met-free media (Sigma-Aldrich) for 1 h. Cells were washed in PBS, lysed in 2 $\times$  Laemmli sample buffer, and equal amounts of protein were separated by SDS-PAGE. Gels were stained with Coomassie (and imaged to ensure equal loading), dried under vacuum, exposed to a storage phosphor screen, and analyzed by phosphorimager analysis.

## Results

### *ISG15-knockout A549 cells recapitulate ISG15-deficient patient cells*

Among the several immune modulatory roles of ISG15 (8), intracellular ISG15 expression, at least in human cells, is critical for regulating the magnitude of the type I IFN response (10, 14). To investigate the pleiotropic nature of human ISG15, we developed cell lines that lack ISG15 expression. Because of our interest in respiratory viruses, including paramyxoviruses, we chose to knockout ISG15 expression in the lung adenocarcinoma cell line A549 by CRISPR/Cas9 genome editing, as described previously (18). Furthermore, A549 cells have proved to be a very useful model for understanding virus-IFN interactions. The resulting culture was single-cell cloned, and ISG15 expression was assessed by immunoblotting three clones (B8, B6, and C4). We also selected a clone that had gone through the CRISPR/Cas9 process but retained ISG15 expression (C4+) (Fig. 1A). In addition to control A549 cells, all clones were treated with IFN- $\alpha$  for 24 or 48 h or left untreated. Immunoblot analysis showed that, compared with control cells, expression of the ISGs MxA and IFIT1 were higher in A549-*ISG15*<sup>-/-</sup> cells (Fig. 1A). It was previously reported that increased ISG expression in ISG15-deficient cells was due to enhanced signaling resulting from the destabilization of the type I IFN negative regulator USP18. To determine if IFN- $\alpha$  treatment led to enhanced signaling in A549-*ISG15*<sup>-/-</sup> cells, we selected clone B8 for further analyses. Cells were treated with IFN- $\alpha$  for 30 min, extensively washed, and media without IFN- $\alpha$  were replaced. Immunoblot analysis of cell lysates taken after 30-min treatment (and following washes; 0 min) and 30 min later showed that IFN- $\alpha$  treatment led to the phosphorylation of STAT1, an indicator of IFN signaling, in both A549 and A549-*ISG15*<sup>-/-</sup> cells (Fig. 1B). Following 24 h treatment, there was clear evidence of ISG expression, as shown by the expression of MxA and ISG15 (in A549 cells) and enhanced expression of STAT1 (Fig. 1B). However, whereas phospho-STAT1 levels had abated in both cell lines 24 h after IFN- $\alpha$  treatment, levels were clearly higher in A549-*ISG15*<sup>-/-</sup> cells, indicating that in these cells, there was a higher degree of signaling. We also tested the impact of ISG15 deficiency on the expression of various ISG mRNAs. A549-*ISG15*<sup>-/-</sup> cells were, in addition to control A549 cells, treated with IFN- $\alpha$  or left untreated for 24 h, and the expression of various ISGs were examined by reverse transcription quantitative PCR. Whereas IFN- $\alpha$  treatment enhanced the expression of all ISGs tested, this increase was larger in ISG15-deficient cells compared with control A549 cells (between 5- and 10-fold, depending on the ISG) (Fig. 1C). Importantly, the expression of ISGs in nonstimulated cells was equivalent to control cells, suggesting that

ISG15-dependent regulation is specific to the IFN response and not required for the regulation of basal gene expression. Further experiments showed that lack of ISG15 prolonged the longevity of ISG protein expression, which presumably has an impact on patients with autoinflammatory diseases associated with ISG15 loss of function. In this study, control A549 and knockout cells were treated with IFN- $\alpha$  for 24 h. The cells were washed, and media (without IFN- $\alpha$ ) were then added. Cells were harvested every 24 h for 72 h, and MxA expression was assessed by immunoblotting (Fig. 1D). In control A549 cells, MxA expression peaked at 24 h (the point at which IFN was removed) and had returned to basal levels between 48 and 72 h. In knockout cells, MxA expression was clearly higher than in control cells, corroborating our mRNA analyses. Furthermore, whereas MxA expression in A549-*ISG15*<sup>-/-</sup> did recede between 48 and 72 h, high protein levels remained at 72 h (Fig. 1D). A dysregulated IFN response in ISG15-deficient cells is thought to be due to destabilization of USP18, a known negative regulator of JAK/STAT signaling (10). To determine if USP18 is similarly affected in our cell lines, A549-*ISG15*<sup>-/-</sup> cells were treated with IFN- $\alpha$  for 24 or 48 h (or left untreated), and whole-cell lysates were probed for USP18 by immunoblotting. USP18 was robustly induced in A549 cells following IFN- $\alpha$  treatment; however, levels of USP18 were much lower in IFN- $\alpha$ -treated ISG15-deficient cells (Fig. 1E). *USP18* mRNA levels were ~10-fold higher in IFN-treated ISG15-deficient cells compared with control A549s, demonstrating that reduced USP18 in A549-*ISG15*<sup>-/-</sup> cells was not due to reduced transcription (Fig. 1C). Together, these data show that ISG15 is critical for the regulated expression of ISGs. Moreover, they demonstrate that the effects of IFN treatment on our ISG15 knockout A549 cell lines recapitulate the findings in cells derived from ISG15-deficient patient cells.

### *ISG15 deficiency leads to translational repression following IFN treatment*

During our studies, we observed that IFN- $\alpha$  treatment of ISG15-knockout cells led to a reduction in protein synthesis and reasoned that this was a likely contributor to the reported virus resistance in ISG15-deficient cells (14). To investigate this, we treated, or left untreated, A549 and A549-*ISG15*<sup>-/-</sup> (B8) cells with IFN- $\alpha$ . At 24, 48, and 72 h following treatment, cells were pulse labeled with <sup>35</sup>S-Met for 1 h, and the incorporation of <sup>35</sup>S-Met was analyzed by phosphorimager analysis. These data showed, compared with control cells, that there was a pronounced decrease in protein synthesis in ISG15<sup>-/-</sup> cells between 24 and 48 h (Fig. 2A). We also investigated whether this decrease in protein synthesis would lead to the inhibition of viral protein synthesis. Cells were pre-treated with IFN- $\alpha$  for 8 h or left untreated, infected with the orthorubulavirus PIV5 (family *Paramyxoviridae*, subfamily *Orthorubulavirinae*) at an MOI of 10 and then labeled for 1 h with <sup>35</sup>S-Met at 24 and 48 h p.i. (32 and 56 h after IFN- $\alpha$  treatment, respectively). Because of the abundance of viral proteins in infected cells, they can be observed by phosphorimager analysis, which following a 1-h treatment of infected cells with <sup>35</sup>S-Met at 24 and 48 h p.i., showed higher levels of newly synthesized viral protein at 24 h p.i. than at 48 h p.i. in A549 cells (Fig. 2B). This is because peak viral transcription occurs between 18 and 24 h p.i. (26). This differs from immunoblot analysis that measures the accumulation of viral protein over time; in this study, the levels of viral protein appeared as high, if not higher, at 48 h p.i. than 24 h p.i. (Fig. 2C). In contrast, the levels of viral protein synthesis following IFN- $\alpha$  treatment was higher at 48 h p.i. than at 24 h p.i. because IFN- $\alpha$  treatment delayed PIV5 infection (Fig. 2B). This was also indicated by immunoblot analysis in which the accumulation of NP was higher at 48 h p.i. than 24 h p.i. (Fig. 2C).

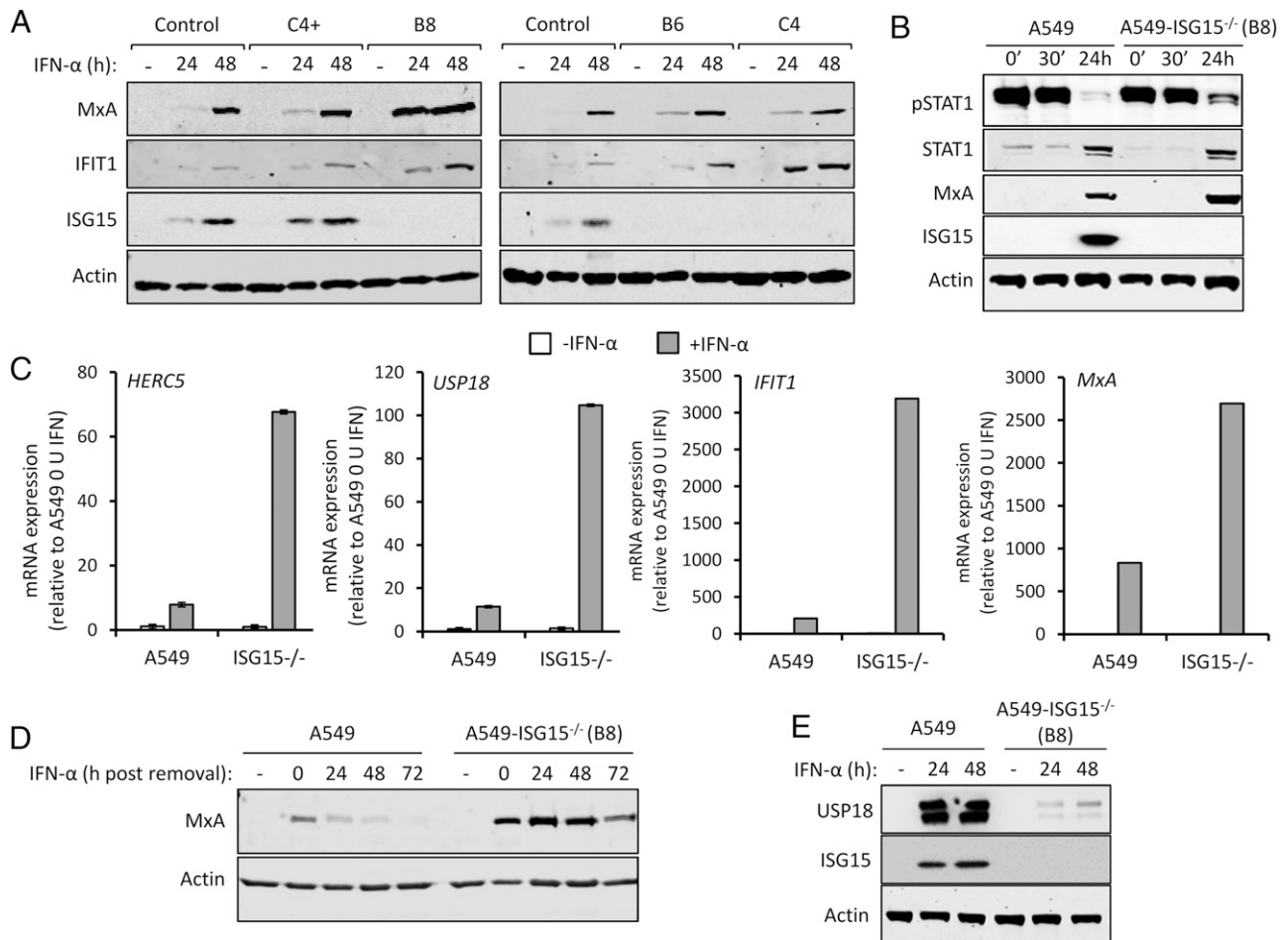


**FIGURE 1.** Functional characterization of A549-ISG15-knockout cell lines. **(A)** CRISPR/Cas9 genome editing was used to knockout ISG15 expression in A549 cells, followed by single-cell cloning [following previously reported procedures (18)]. Four independent clones were treated with 1000 IU/ml IFN- $\alpha$  for 24 and 48 h or left untreated, and protein expression was tested by immunoblot analysis of ISG15, MxA, IFIT1, and  $\beta$ -actin. Control cells were naive A549 cells. Representative image from two independent experiments. **(B)** A549 and A549-ISG15<sup>-/-</sup> (B8) cells were treated with 1000 IU/ml IFN- $\alpha$  for 30 min, then extensively washed and media without IFN replaced. Cells were harvested at 0 and 30 min and 24 h after IFN- $\alpha$  removal and phospho-STAT1, total STAT1, MxA, ISG15, and  $\beta$ -actin were detected following immunoblot analysis. **(C)** A549 and A549-ISG15<sup>-/-</sup> (clone B8) were treated with 1000 IU/ml IFN- $\alpha$  for 24 h. Expression of ISGs was tested using reverse transcription quantitative PCR (RT-qPCR) with primers specific for *HERC5*, *USP18*, *IFIT1*, and *MxA*. Relative expression was determined following SYBR Green quantitative PCR (qPCR) using  $\Delta\Delta C_t$  method.  $\beta$ -Actin expression was used to normalize between samples. Error bars represent the SD of the mean from three independent RNA samples. **(D)** A549 and A549-ISG15<sup>-/-</sup> (clone B8) were treated with 1000 IU/ml for 24 h. Cells were washed, and fresh media (without IFN- $\alpha$ ) were replaced. Cells were processed for immunoblot analysis using Abs specific for MxA and  $\beta$ -actin at 24 h post-IFN- $\alpha$  and every 24 h thereafter for 72 h. Controls were cells without IFN- $\alpha$ . Representative image from two independent experiments. **(E)** A549 and A549-ISG15<sup>-/-</sup> (clone B8) were treated with 1000 IU/ml for 24 and 48 h (or left untreated). Whole-cell lysates were analyzed by immunoblotting with Abs specific for USP18, ISG15, and  $\beta$ -actin. Image is representative of more than three independent experiments.

When A549-ISG15<sup>-/-</sup> cells were infected, there was clear evidence of NP protein synthesis (Fig. 2B) and accumulation (Fig. 2C); however, when these cells were pretreated with IFN- $\alpha$  and infected, there was very little evidence of viral protein synthesis (Fig. 2B) or accumulation (indicating that viral protein synthesis was barely initiated) (Fig. 2C) at any time p.i. These data demonstrate that IFN- $\alpha$  treatment of A549-ISG15<sup>-/-</sup> cells led to inhibition of protein synthesis that was associated with viral resistance, at least at later times.

#### *Pretreatment of ISG15-deficient cells with IFN- $\alpha$ renders them resistant to PIV infection*

Previous studies have shown that IFN- $\alpha$  treatment of ISG15-deficient patient cells renders them resistant to viral infection by several viruses, including the murine respirovirus (family *Paramyxoviridae*, subfamily *Orthoparamyxovirinae*) Sendai virus (14), and this seems to extend to PIV5 with our in vitro system (Fig. 2B, 2C). To investigate this in A549-ISG15<sup>-/-</sup> cells, control A549 cells and the ISG15 knockout clones described above were

either untreated or treated with 1000 IU/ml IFN- $\alpha$ 2b [the same concentration and IFN- $\alpha$  type used in (14)] for 18 h. Cells were then infected with PIV5 (PIV5-W3) (22) for 24 and 48 h and analyzed by immunoblotting. In all cell lines, the levels of PIV5 NP expression was equivalent at 24 and 48 h in unstimulated cells (Fig. 3A). In IFN- $\alpha$ -pretreated control cells, including C4+ that retained ISG15 expression, the level of NP expression was markedly reduced at 24 h. By 48 h, the level of NP increased, showing that infection had progressed even in the presence of IFN- $\alpha$  (Fig. 3A). This is because the PIV5-V protein targets STAT1 for proteasomal degradation, and once sufficient V is expressed, the IFN response is dismantled, allowing the virus to replicate (23). Indeed, there was no detectable STAT1 and, as a result, markedly reduced levels of ISGs MxA and IFIT1 in PIV5-infected, ISG15-expressing cells (Fig. 3A). However, all A549-ISG15<sup>-/-</sup> cell lines that had been pretreated with IFN- $\alpha$  were resistant to PIV5 infection, as shown by dramatically reduced, or even absent, NP expression at both time points (Fig. 3A). Moreover, these cells

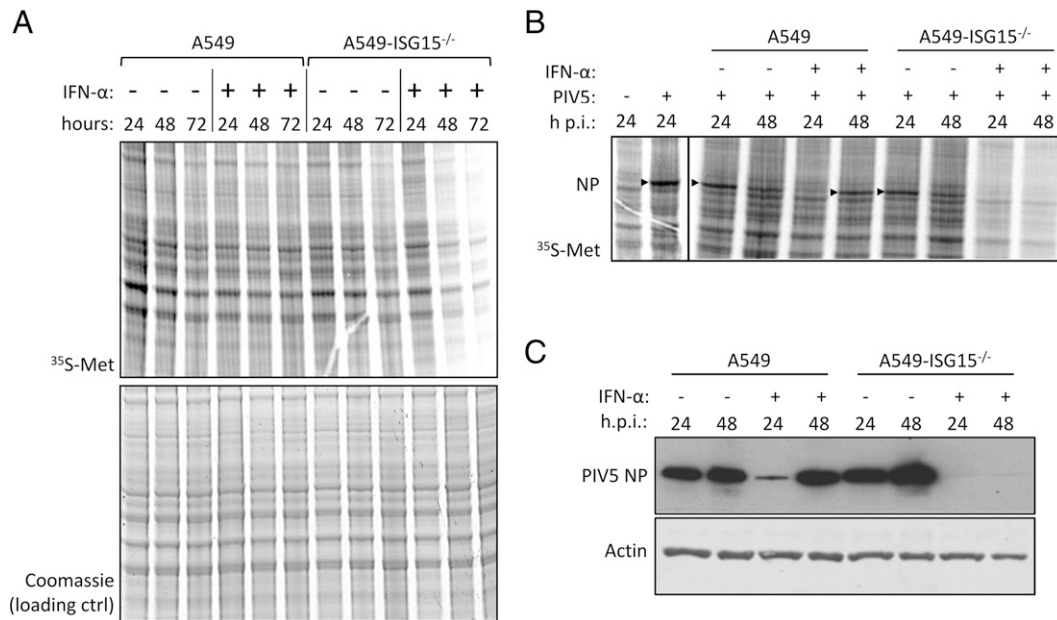


**FIGURE 2.** Analysis of cellular and viral protein synthesis in ISG15-deficient cells during an antiviral state. **(A)** Subconfluent A549 and A549-ISG15<sup>-/-</sup> (B8) cells were treated with 1000 IU/ml IFN-α or left untreated. At 24, 48, and 72 h, cells were pulsed for 1 h with L-<sup>35</sup>S-Met in Met-free media to metabolically label nascent proteins. Proteins were resolved by SDS-PAGE and stained with Coomassie to ensure equal loading. Labeled proteins were visualized by phosphorimager analysis. **(B)** A549 and A549-ISG15<sup>-/-</sup> (B8) cells were treated with 1000 IU/ml IFN-α for 8 h or left untreated and then infected with PIV5-W3 (MOI = 10). At 24 or 48 h p.i., cells pulsed and processed as in (A). Arrow heads denote <sup>35</sup>S-Met-labeled PIV5 NP. Both experiments were performed independently at least twice. **(C)** PIV5-infected lysates from (B) were immunoblotted, and the accumulations of PIV5 NP and β-actin were detected with specific Abs and HRP-conjugated secondary Abs.

displayed STAT1 expression and the expression of associated MxA and IFIT1 (indicating that PIV5 infection was inhibited) (Fig. 3A).

Previous reports have shown that the ISG15 regulation of IFN signaling is independent of its ability to covalently modify proteins by ISGylation (10). To confirm this, we again applied CRISPR/Cas9 genome engineering technology and knocked out expression of UBA7, the E1 enzyme required for ISGylation. For this, we took a different approach compared with generating our ISG15-knockout cells (19). In this study, we introduced constitutive expression of Cas9 by lentiviral transduction of A549 cells and transduced A549-Cas9 cells with lentiGuide-Puro lentivirus carrying a guide RNA specific for UBA7, followed by single-cell cloning. We confirmed that all clones were UBA7 deficient by immunoblot analysis, which demonstrated that they retained expression of ISG15 but had lost the ability to ISGylate proteins (Fig. 3B). Additionally, following the scheme used in Fig. 3A, these cells were infected with PIV5-W3. These data showed that, compared with ISG15 knockout cells that were resistant to infection, all IFN-α-pretreated UBA7-knockout cells were infected as efficiently as control cells (Fig. 3B), confirming reports that ISG15-dependent regulation of type I IFN signaling does not require ISGylation (10).

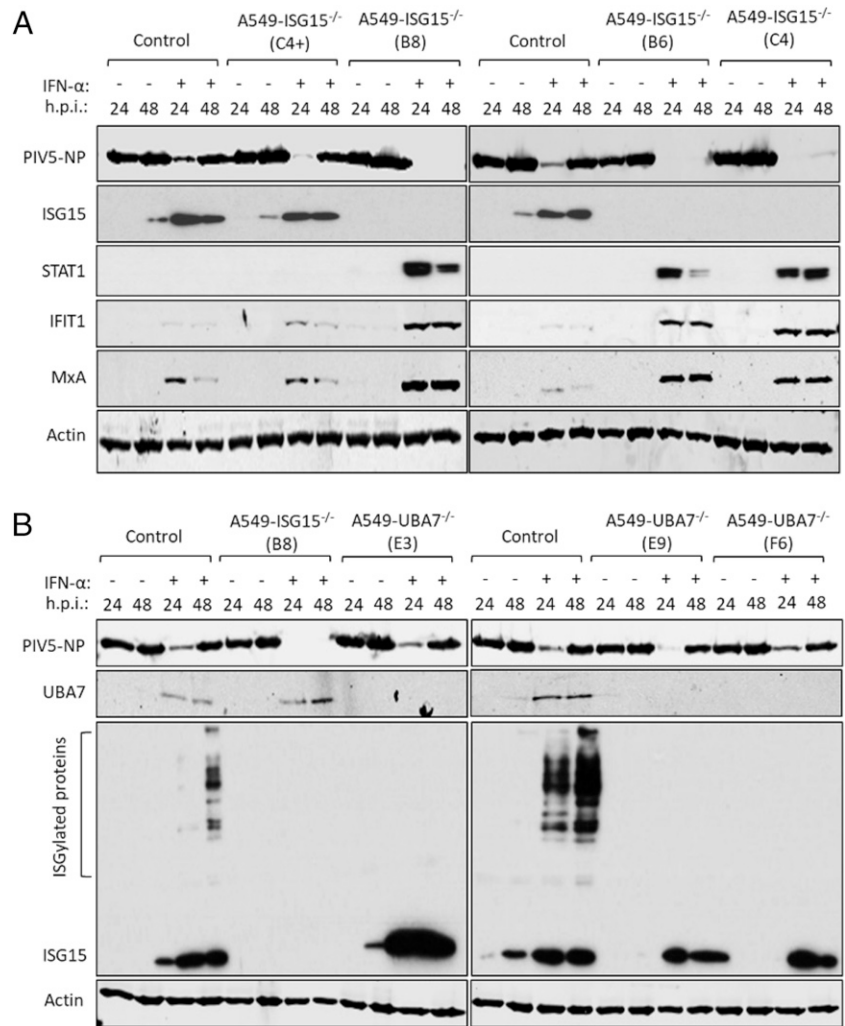
#### *The direct antiviral activity of ISGs is responsible for virus resistance*

Virus resistance can be induced following 8-h IFN-α treatment (shorter times were not tested) well before any obvious effect on global protein synthesis (Fig. 2). Therefore, shutdown of translation is unlikely to be the sole contributor to virus resistance at early time points, and so, we wished to determine whether the direct antiviral activity of ISGs was responsible. Addressing this question is complex because, for most viruses, the specific ISG(s) responsible for blocking replication is not known. However, for PIV5, it has been established that IFIT1 is the principle ISG

responsible for most of the IFN-dependent antiviral activity (17, 27). We therefore hypothesized that if virus resistance was caused by the direct antiviral activity of ISGs, knockdown of IFIT1 in ISG15-deficient cells would permit PIV5 replication during an antiviral response. We reduced IFIT1 [according to (17)] in A549 and A549-ISG15<sup>-/-</sup> cells, and all four cell lines (A549, A549-ISG15<sup>-/-</sup>, and the respective shIFIT1 cells) were pretreated, or left untreated, with IFN-α and then infected with PIV5-W3 (MOI 10) for 24 and 48 h. Expression of PIV5 NP, analyzed by semiquantitative immunoblotting, was used to measure virus infection (Fig. 4A). IFIT1 levels and expression of ISG15 were likewise tested. Typically, pretreatment of naive cells with IFN-α reduced infection, as shown by a reduction in NP levels, compared with nontreated cells (Figs. 2B, 2C, 3); nevertheless, because PIV5 expresses the IFN antagonist V protein, NP levels reach similar levels to untreated cells by 48 h p.i. However, this IFN-dependent reduction in virus infection is diminished when IFIT1 is knocked down, confirming earlier reports of IFIT1's antiviral activity against PIV5 (17, 27). Although IFN-α pretreatment of A549-ISG15<sup>-/-</sup> cells renders them resistant to infection, when IFIT1 was also knocked down, PIV5 infection was restored (Fig. 4A). Because we performed semiquantitative immunoblotting of NP and β-actin, we were able to quantify NP levels, allowing us to analyze these changes statistically (Fig. 4B). These data show that in IFN-α-pretreated cells, knocking IFIT1 down restored NP to similar levels to those seen in untreated cells, regardless of ISG15 status. Although IFN-α pretreatment of A549 cells significantly reduced NP levels when we compared 24 and 48 h p.i. samples, there was no difference at these time points when IFIT1 was knocked down (Fig. 4B). Importantly, although NP levels were virtually absent in IFN-α-pretreated ISG15-deficient cells, when IFIT1 was knocked down in these cells, NP levels were equivalent to A549-shIFIT1 cells (Fig. 4B).

Rather than solely relying on viral protein expression as a surrogate for virus infection, we also tested virus replication using

**FIGURE 3.** IFN- $\alpha$  pretreatment of ISG15-deficient cells leads to virus resistance that is independent of ISGylation. **(A)** Control (naive A549) and four independent clones of A549-ISG15<sup>-/-</sup> cells generated by CRISPR/Cas9 genome editing were treated with 1000 IU/ml IFN- $\alpha$  for 16 h or left untreated and then infected with PIV5-W3 (MOI = 10). Cells were harvested at 24 and 48 h p.i. and processed for immunoblot analysis using Abs specific for PIV5 NP, ISG15, STAT1, IFIT1, MxA, and  $\beta$ -actin. This experiment was independently performed twice. **(B)** UBA7-knockout cells were generated using CRISPR/Cas9 genome editing; Cas9-expressing A549 cells were first generated (following transduction with lentiCas9-Blast) and then transduced with lenti-Guide-Puro expressing a sgRNA that targeted exon 3 of the UBA7 gene. Knockout cells were single-cell cloned, and three were selected for further analysis. These cells were treated with IFN- $\alpha$  or left untreated, infected, and processed as in (A) using Abs specific for PIV5 NP, ISG15, UBA7, and  $\beta$ -actin. This experiment was independently performed twice.



biologically relevant plaque assays. Because paramyxoviruses (like most wild-type viruses) are poor inducers of the IFN response (28, 29), are able to efficiently and rapidly counteract it if it were induced, and our data showed that basal ISG expression was not effected in ISG15-deficient cells (Fig. 1C), we predicted that infection of naive A549-ISG15<sup>-/-</sup> cells would be equivalent to naive A549 cells. To determine if this was the case, plaque assays were performed with various paramyxoviruses. These data show that each virus formed plaques that were analogous on both A549 and A549-ISG15<sup>-/-</sup> cells (Supplemental Fig. 1). There were subtle differences in plaque phenotype; for instance, infection of ISG15-deficient cells, particularly with HPIV2 but also evident following PIV5 infection, resulted in plaques with poorer defined edges (hazy plaques) (Supplemental Fig. 1). The reason for this is currently not clear but may indicate an antiviral role for ISG15 against HPIV2 and PIV5. Nevertheless, this, and data in Figs. 2 and 3, supports the notion that naive cells were not resistant to wild-type viral infection. However, viruses unable to counteract the IFN response should be restricted and therefore provide a means of assessing the role of ISG15 and virus resistance.

To do this, cells were infected with ~30–40 PFU of PIV5-CPI<sup>-</sup> (30), a strain unable to block IFN signaling because of a mutation in its V protein. Infected cells were fixed 6 d p.i. and stained for viral Ag (Fig. 4C). As previously demonstrated (17), PIV5-CPI<sup>-</sup> was unable to efficiently form plaques in IFN-competent A549 cells. However, PIV5-CPI<sup>-</sup> did replicate when cells were unable to produce IFN, such as in A549-Npro cells that constitutively

express bovine viral diarrhea virus Npro that targets IRF3 for degradation [a transcription factor critical for IFN induction (21)]. Furthermore, when IFIT1 was knocked down, PIV5-CPI<sup>-</sup> was able to replicate (albeit less efficiently), further highlighting the major role of IFIT1 as an anti-PIV5 protein. As expected, and like A549 cells, there was very little virus replication in A549-ISG15<sup>-/-</sup> cells; however, when IFIT1 was knocked down, cells were able to support virus replication. It must be noted, however, that virus replication in A549-ISG15<sup>-/-</sup>/shIFIT1 cells did not recover to the same degree as A549-shIFIT1 cells. We propose that the reason for this will be complex and may include the likelihood that additional, yet-to-be-identified anti-PIV5 ISGs exist that are expressed at higher levels in ISG15-deficient cells. Another possible explanation is the inhibition of protein synthesis, including that of viral proteins, in ISG15-deficient cells; cells were infected for 6 d prior to performing the plaque assays, a time point beyond that required to observe a significant effect on protein synthesis (Fig. 2A). Therefore, the plaques observed in A549-ISG15<sup>-/-</sup>/shIFIT1 cells likely result from virus that replicated prior to the inhibition of global protein synthesis.

IFIT1 restricts viral infection posttranscriptionally by blocking the translation of viral mRNA (17, 27); therefore, we predicted that IFN- $\alpha$ -pretreated A549-ISG15<sup>-/-</sup> cells would remain susceptible to infection but that high levels of IFIT1 would mean these cells would not be permissive to PIV5 infection. Furthermore, investigating this could highlight additional restrictions to viral infection, such as entry. A549 and A549-ISG15<sup>-/-</sup> cells were pretreated for

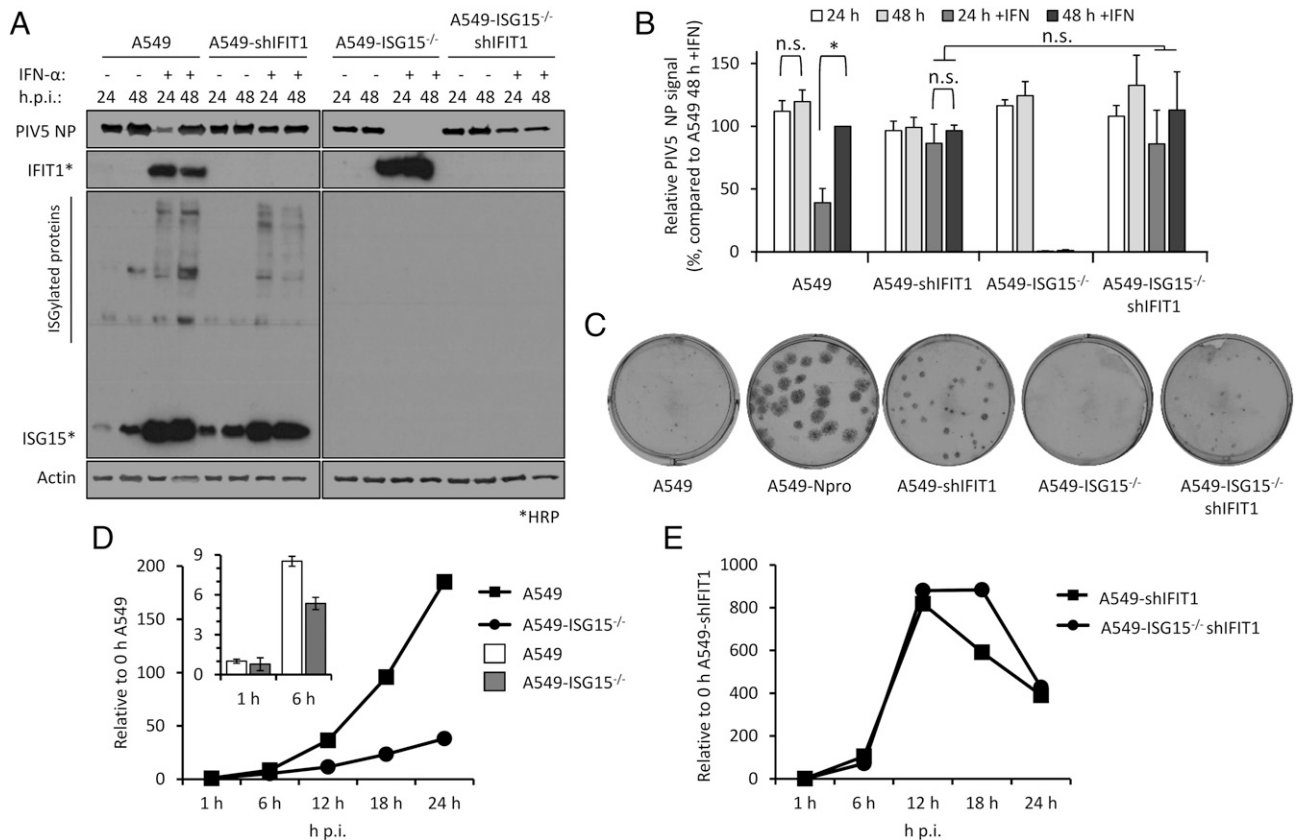


**FIGURE 4.** Direct antiviral activity of ISGs is responsible for virus resistance because of ISG15 loss of function. **(A)** IFIT1 was constitutively knocked down in A549 or A549-ISG15<sup>-/-</sup> (B8) cells following a previously described method (17). A549, A549-ISG15<sup>-/-</sup> (B8), and the corresponding IFIT1-knockdown cells were treated with IFN- $\alpha$ , infected with PIV5, and processed as in Fig. 3A. Following immunoblotting with specific Abs, PIV5 NP and  $\beta$ -actin were detected using near-infrared (NIR) dye-conjugated secondary Abs to facilitate quantification. IFIT1 and ISG15 proteins were detected using chemiluminescence following incubation with HRP-conjugated secondary Abs. **(B)** Experiments described in (A) were performed independently three times (infections were performed on three separate occasions), and NP and  $\beta$ -actin levels were quantified using Image Studio software (LI-COR Biosciences). Signals were relative to those generated from IFN- $\alpha$ -treated A549 cells infected for 48 h p.i. (set to 100%). Error bars represent the SD of the mean from the three independent experiments performed on different occasions. \* $p < 0.05$ , using two-way ANOVA and Tukey multiple comparisons test. n.s., no statistical significance. **(C)** Indicated cells were infected for 1 h with 30–40 PFU of PIV5 (CPI<sup>+</sup>), a strain unable to block the IFN response because of mutation in the viral V protein. Monolayers were fixed 6 d p.i. Plaques were detected using a pool of anti-PIV5 Abs specific for hemagglutinin (HN), NP, P, and matrix protein (M) [see (24)]. Plaque assays were performed on three independent occasions. **(D)** A549 and A549-ISG15<sup>-/-</sup> cells were infected with PIV5 W3 (MOI 10) and harvested at the indicated times. Total RNA was isolated and subjected to cDNA synthesis using oligo(dT) primers. Expression of PIV5 NP was measured using quantitative PCR (qPCR). Relative expression (compared with 1-h A549) was determined following SYBR Green qPCR using  $\Delta\Delta C_t$  method.  $\beta$ -Actin expression was used to normalize between samples. Error bars represent the SD of the mean from three independent RNA samples. For clarity, the inset bar graph represents viral transcription data at 1 and 6 h p.i. only. **(E)** Analyses followed that of (D), but A549-shIFIT1 and A549-ISG15<sup>-/-</sup>/shIFIT1 cells were infected.

8 h with IFN- $\alpha$  and then infected with PIV5-W3 (MOI 10) (Fig. 4D). Analysis of PIV5 NP transcription showed that ISG15-deficient cells were infected and that viral transcription increased over time; however, this was muted compared with A549 control cells. Importantly, however, the levels of NP transcription at 1 h p.i. was equivalent in both cell lines, a time point that likely represents primary transcription (Fig. 4D; see inset graph). These data suggest that both cell lines were susceptible to infection and that high levels of pre-existing IFIT1 strongly restricted further viral transcription by preventing the translation of the virally encoded mRNAs. To investigate if IFIT1 restriction was responsible for reduced viral transcription in ISG15-deficient cells, we repeated the experiment in A549-shIFIT1 and A549-ISG15<sup>-/-</sup>/shIFIT1 cells (Fig. 4E). These data show that in IFN- $\alpha$ -treated cells, viral transcription was markedly increased compared with cells with intact IFIT1 expression. Furthermore, in A549-shIFIT1 cells, transcription peaked between 12 and 18 h p.i. and then receded. We have recently described the transcription and replication of various paramyxoviruses, including PIV5-W3,

using unbiased high-throughput, RNA-sequencing approach (26); this report shows that this pattern of transcription is typical of PIV5-W3 and likely results from the P-dependent repression of viral transcription and replication (31). This repression also occurred in A549-ISG15<sup>-/-</sup>/shIFIT1 cells, but this occurred later (Fig. 4E), suggesting that ISG15 may be an additional antiviral factor that curtail PIV5 transcription. Nevertheless, these data showed that when IFIT1 levels were knocked down, the transcriptional repression identified in IFN- $\alpha$ -pretreated ISG15-deficient cells was relieved, demonstrating that virus resistance was due to the posttranscriptional activity of IFN-inducible IFIT1. We also investigated infection of these cell lines with other paramyxoviruses whose sensitivity to IFIT1 has been previously reported. Cells were treated with IFN- $\alpha$  and then infected with HPIV2 strain Colindale (MOI 10; family *Paramyxoviridae*, subfamily *Orthorubulavirinae*), which is reported to be moderately sensitive to IFIT1 restriction (27) for 24 and 48 h (untreated cells were not analyzed because of high cytopathic effect in the absence of IFN). To investigate infection, we

detected expression of HPIV2 P by semiquantitative immunoblotting (Fig. 5A), which showed that IFN- $\alpha$ -pretreated A549-ISG15<sup>-/-</sup> cells were largely resistant to infection, although by 48 h p.i., there was some, albeit low-level, evidence of viral protein accumulation. Nevertheless, infection of A549-ISG15<sup>-/-</sup>/shIFIT1 did allow significantly more viral protein expression. Semiquantitative analyses demonstrated that viral protein accumulation in A549-ISG15<sup>-/-</sup>/shIFIT1 cells was significantly higher than in A549-ISG15<sup>-/-</sup> cells, but this was not as high as in A549 control cells, which agrees with the reported partial sensitivity of HPIV2 to IFIT1 restriction, indicating that additional ISGs target HPIV2 (Fig. 5B). We performed a similar analysis with HPIV3 strain Washington (20) (family *Paramyxoviridae*, subfamily *Orthoparamyxovirinae*), a virus reported to have limited sensitivity to IFIT1 (27). Interestingly, pretreatment of A549 and A549-shIFIT1 cells with IFN- $\alpha$  had less of an effect on virus protein accumulation compared with the effects on PIV5 infection (Fig. 5C). Furthermore, whereas infection of IFN- $\alpha$ -pretreated ISG15-knockout cells significantly reduced infection compared with control cells, virus infection in these cells was still more robust compared with PIV5 and HPIV2-infected cells. Nevertheless, knockdown of IFIT1 only slightly increased HPIV3 protein expression in both ISG15-competent and ISG15-deficient

cells (Fig. 5D), supporting reports of a minor role of IFIT1 during the antiviral response to HPIV3 (27).

*ISG15-deficient cells pretreated with IFN- $\alpha$  for longer times were resistant to infection independently of the direct antiviral activity of IFN-dependent restriction factors*

Our data have so far suggested that early virus resistance is mediated by the direct antiviral activity of the IFN response. However, protein synthesis is reduced at later times after IFN treatment, and this is likely to cause resistance; therefore, we investigated whether PIV5 resistance could be induced independently of the direct antiviral activity of IFIT1. To do this, we pretreated the four cell lines (A549, A549-shIFIT1, A549-ISG15<sup>-/-</sup>, and A549-ISG15<sup>-/-</sup>-shIFIT1) with IFN- $\alpha$  for different periods of time, infected with a recombinant PIV5 that expresses the fluorescent protein mCherry (rPIV5-mCherry) for 48 h (MOI 10) and measured fluorescence as a marker of virus replication (Fig. 6A). Virus replication in A549 cells was equivalent regardless of the time cells had been pretreated with IFN- $\alpha$ , and as expected, A549-ISG15<sup>-/-</sup> cells were resistant to infection at any time after IFN- $\alpha$  treatment (Fig. 6B). Any advantage to PIV5 replication as a result of IFIT1 knockdown in A549-shIFIT1 cells was lost when cells had been pretreated for 16 h or more, as longer periods of pretreatment

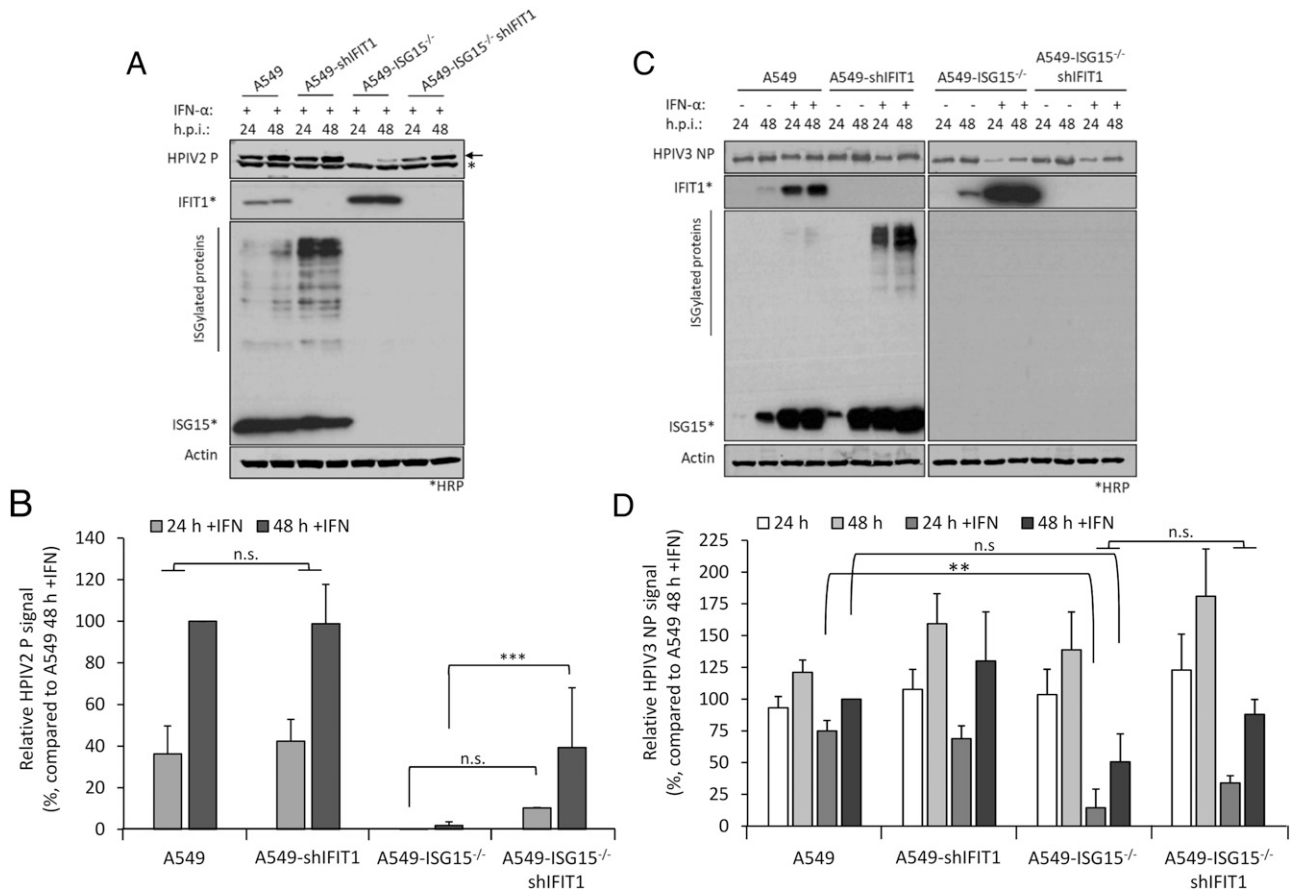


**FIGURE 5.** Restoration of paramyxovirus infection in IFN- $\alpha$ -pretreated ISG15<sup>-/-</sup> cells reflects their reported sensitivity to IFIT1. (**A** and **B**) Experiments were performed as in Fig. 4A and 4B. (A) HPIV2 proteins were detected with Abs specific for HPIV2 P [clone 161 (24)] and NIR-conjugated secondary Abs. Single asterisks (\*) denote detection of an irrelevant protein, and arrow denotes HPIV2 P. Samples not treated with IFN- $\alpha$  were omitted due to the highly lytic nature of HPIV2, which hampered their accurate quantification. (B) Quantification of normalized NP signals and compared with the 48 h p.i. sample that was set to 100%. (C) HPIV3 NP proteins were detected using Abs specific for HPIV3 NP and NIR-conjugated secondary Abs. (D) Normalized signals were quantified as in (B) and compared with IFN- $\alpha$ -treated, 48-h p.i. samples (set to 100%). Means and SD were derived from five independent experiments for HPIV2 and four independent experiments (for HPIV3) performed on different occasions. \*\* $p < 0.01$ , \*\*\* $p < 0.001$ , using two-way ANOVA with Tukey multiple comparison test (for HPIV3) and one-way ANOVA with Sidak multiple comparisons test (for HPIV2). n.s., no statistical significance.

resulted in replication equivalent to IFN-pretreated A549 cells. Similarly, PIV5 replication in A549-ISG15<sup>-/-</sup>-shIFIT1 cells was higher than A549 control cells and equivalent to A549-shIFIT1 cells following 8 and 16 h pretreatment; however, when cells were pretreated for 24 h, replication was lower than in A549 and A549-shIFIT1 cells. Interestingly, as the time of pretreatment of A549-ISG15<sup>-/-</sup>-shIFIT1 cells extended, virus replication reduced further until cells became resistant (e.g., at 60 and 72 h pretreatment, Fig. 6B), which was not observed in A549 or A549-shIFIT1 cells. These data suggest that cell permissiveness progressively reduced with longer times of IFN- $\alpha$  pretreatment, which correlated with the effects of IFN- $\alpha$  treatment on protein synthesis in ISG15-deficient cells (Fig. 2).

A previous report demonstrated that ISG15-dependent stabilization of USP18 was required to bring about regulation of the type I IFN response, and this was sufficient for these cells to once again be infected (14). However, what aspects of the antiviral response was responsible for resistance was not investigated. Taken together, these data strongly suggest that virus resistance in early IFN-treated ISG15-deficient cells was caused by the direct antiviral activity of ISGs and not because of a lack of permissiveness as a result of IFN-dependent inhibition of protein synthesis. Nevertheless, because of the reduced protein synthesis in IFN- $\alpha$ -treated ISG15-deficient cells, cells later become nonpermissive to infection, even when key ISGs are eliminated.

## Discussion

Previous work had shown that virus resistance was observed in ISG15-deficient cells that had been treated with IFN- $\alpha$  and then left to rest for 36 h prior to challenge (14). We had observed that IFN- $\alpha$  treatment of A549-ISG15<sup>-/-</sup> cells led to dramatic decreases in protein synthesis, particularly between 24 and 48 h; therefore, it was not clear whether the initially reported virus resistance was due to defects in translation (including of viral mRNAs) at the timepoint used in (14) or due to the direct antiviral activity of the IFN response. For most viruses, the specific ISG(s) with antiviral activity for a given virus is not known, making the latter difficult to discern; however, for PIV5, it is well established that IFIT1 is responsible for the majority of the antiviral response (17). To study this, we generated A549-ISG15<sup>-/-</sup> cells and showed these cells recapitulated the effects observed in ISG15-deficient patient

cells following treatment with IFN- $\alpha$ , which included dysregulated ISG expression and reduced USP18 protein levels following IFN- $\alpha$  treatment (Fig. 1). Additionally, by knocking out UBA7, the first enzyme in the ISGylation cascade, we showed that ISGylation is not required for a regulated response (Fig. 3B), confirming previous reports that free ISG15 is required for regulation (10).

Using these cell lines in combination with a PIV5 infection model, we showed that infection of IFN- $\alpha$ -pretreated ISG15-deficient cells in which IFIT1 had been knocked down restored infection, thus confirming that at early times p.i., resistance was indeed due to the direct antiviral activity of the IFN response. Furthermore, because IFIT1 blocks the translation of viral transcripts, our data show that IFN-treated A549-ISG15<sup>-/-</sup> cells were still susceptible to infection, allowing viral transcription to take place prior to IFIT1 restriction and that ISG15 was unlikely to significantly regulate processes involved in entry (Fig. 4D, 4E). Nevertheless, if ISG15-deficient cells were treated for longer periods with IFN- $\alpha$  prior to infection, they did become resistant, even when IFIT1 was knocked down, suggesting that at later times, the inhibition of protein synthesis was the principal cause of resistance (Fig. 6). These data suggest that the virus resistance reported by Speer et al. (14) was due to a lack of permissiveness and not a result of the direct antiviral activity of the IFN response, although different cells were used in that study.

The data in this study demonstrate that the mechanism of resistance is likely 2-fold, depending on the duration that cells are exposed to IFN- $\alpha$ . It is not currently possible to know which mechanism is dominant in ISG15-deficient patients, but it is likely to be a combination of both. Nevertheless, virus resistance results from a lack of IFN signaling control—as a consequence of ISG15 loss of function—which would explain why ISG15-deficient patients were not more susceptible to severe infection. This observation, therefore, cannot be used to support the notion that human ISG15 does not possess direct antiviral activity, as proposed (14, 16). It is likely that many viruses will not be sensitive to ISG15-dependent antiviral activity; however, this is true of many antiviral effectors. For example, and as confirmed in this study, IFIT1 strongly restricts PIV5 infection, yet it has reduced activity against HPIV2 and likely no activity against HPIV3 or human respiratory syncytial virus (27). It is also true that several ISGs are often required to limit infection

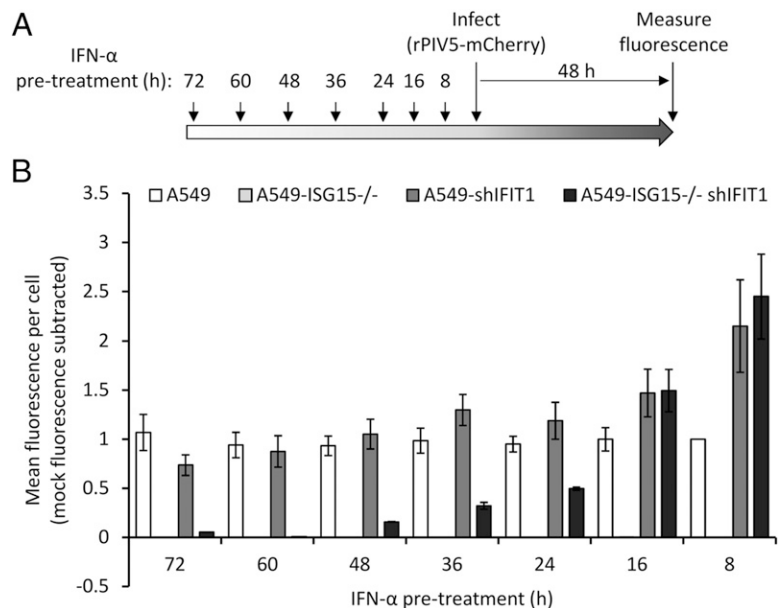


**FIGURE 6.** Virus resistance is induced in ISG15-deficient cells following longer periods of IFN- $\alpha$  pretreatment. **(A)** Experimental workflow. **(B)** Cells were treated 1000 IU/ml IFN- $\alpha$  in six-well plates for the indicated times prior to infection. Pretreated cells were infected with rPIV5-mCherry (MOI 10) for 48 h, and mCherry fluorescence was measured using an IncuCyte ZOOM. Background fluorescence from mock-infected wells was subtracted. Data are representative to two independent experiments.

(6); therefore, if one antiviral effector mechanism is absent (such as ISGylation), there is sufficient redundancy to avoid severe effects of infection (redundancy that can complicate the investigation of specific antiviral mechanisms in *in vitro* studies). Nevertheless, several human viruses have been shown to be sensitive to ISGylation, and many have evolved specific mechanisms to counteract antiviral ISGylation, adding further weight to the argument that human ISG15 does have antiviral activity (reviewed in Ref. 8). Indeed, other than the handful of patients that have been found to lack ISG15 expression (10, 32), individuals will possess an intact IFN response in which the antiviral activity of ISG15 (and other effectors) will function if the infecting virus is sensitive to it.

It was surprising that protein synthesis was so affected in ISG15-deficient cells following IFN treatment. It is well established that inhibition of general protein translation is a key feature of the antiviral response, and this is through the actions of proteins such as PKR or PKR-like ER kinase (PERK) (4). However, for PKR to be activated, it must recognize dsRNA, which was absent in IFN- $\alpha$ -treated cells. Similarly, PERK is activated upon endoplasmic reticulum stress, which might be expected during a viral infection, but not following treatment with IFN alone. Previous reports have shown that carcinoembryonic Ag-related cell adhesion molecule 1 (CEACAM1) has antiviral activity against human CMV, influenza virus, and metapneumovirus by suppressing mTOR-mediated protein synthesis (33, 34). The membrane protein CEACAM1 is induced by innate sensors such as TLR-4 (35) and IFI16 (34) and delivers inhibitory signals via SHP1 (hematopoietic cells) or SHP2 (epithelial and endothelial cells) phosphatase activity through CEACAM1 ITIMs (36). CEACAM1 expression is rapidly induced following activation of NF- $\kappa$ B and IRF1, but whether IFN- $\alpha$  alone (as used in this study) can induce its expression is not clear. The *IRF1* promoter possesses a single GAS element, but no ISRE, and so its expression is induced by STAT1 homodimers (37). Type I IFN signaling predominantly leads to the formation of STAT1-STAT2 heterodimers that associate with IRF9 (to form the ISGF3 transcription factor) to drive expression of ISGs that possess ISRE elements in their promoters; however, STAT1 homodimers are formed after type I IFN treatment, but these are at lower concentrations. It is possible that late inhibition of protein synthesis in ISG15-deficient cells (compared with the swifter antiviral activity of ISRE-containing genes such as IFIT1) may relate to the kinetics of CEACAM1 expression, as the accumulation of STAT1 homodimers is required to drive the expression of *IRF1*, that itself needs to be translated before it induces *CEACAM1*. Of course, the accumulation of STAT1 homodimers may be higher in ISG15-deficient cells because of a dysregulated type I IFN response. Nevertheless, it is plausible that the overamplified type I IFN response in ISG15-deficient cells led to high levels of CEACAM1 (compared with control cells), resulting in inhibition of protein synthesis. Moreover, ISG15 may have yet-to-be-characterized functions in regulating the cellular response to stressors that lead to inhibition of protein synthesis.

It has been reported that ISG15 has a role in regulating the cell cycle through its interactions with SKP2 and USP18, although experiments in that study were not performed in IFN-treated cells, nor were ISG15 knockout cells tested (15). Although rates of protein synthesis differ during different stages of the cell cycle, translation is thought to be lowest during mitosis (38). Perturbation of the ISG15-SKP2-USP18 axis following ablation of USP18 led to a delayed progression from G1 to S phase, which is not generally thought to be associated with translational repression (39). Of note, we have not observed any obvious differences in cell growth in nontreated A549-ISG15<sup>-/-</sup> cells. Further work is required to dissect the mechanism

responsible for ISG15's effects on general protein translation during an antiviral response.

ISG15 has emerged as a central regulator of immunity. It is a pleiotropic protein that is strongly expressed following activation of innate immune sensors and connects innate and adaptive immunity. In this study, we have shown that a lack of ISG15 leads to virus resistance by two kinetically distinct mechanisms; the rapid induction of antiviral ISGs and the unexpected effects on protein synthesis. Our newly developed cell lines and infection model will pave the way for further studies investigating the regulatory mechanisms of ISG15 during the antiviral response.

## Acknowledgments

We acknowledge technical support provided by Christopher Simmons-Riach and Miroslav Botev.

## Disclosures

The authors have no financial conflicts of interest.

## References

- McFadden, M. J., N. S. Gokhale, and S. M. Horner. 2017. Protect this house: cytosolic sensing of viruses. *Curr. Opin. Virol.* 22: 36–43.
- Kawai, T., and S. Akira. 2010. The role of pattern-recognition receptors in innate immunity: update on toll-like receptors. *Nat. Immunol.* 11: 373–384.
- Randall, R. E., and S. Goodbourn. 2008. Interferons and viruses: an interplay between induction, signalling, antiviral responses and virus countermeasures. *J. Gen. Virol.* 89: 1–47.
- Dalet, A., E. Gatti, and P. Pierre. 2015. Integration of PKR-dependent translation inhibition with innate immunity is required for a coordinated anti-viral response. *FEBS Lett.* 589: 1539–1545.
- Mears, H. V., and T. R. Sweeney. 2018. Better together: the role of IFIT protein-protein interactions in the antiviral response. *J. Gen. Virol.* 99: 1463–1477.
- Schoggins, J. W., S. J. Wilson, M. Panis, M. Y. Murphy, C. T. Jones, P. Bieniasz, and C. M. Rice. 2011. A diverse range of erratum products are effectors of the type I interferon antiviral response. [Published erratum appears in 2015 *Nature* 525: 144.] *Nature* 472: 481–485.
- Yu, Z. X., and H. M. Song. 2020. Toward a better understanding of type I interferonopathies: a brief summary, update and beyond. *World J. Pediatr.* 16: 44–51.
- Perng, Y. C., and D. J. Lenschow. 2018. ISG15 in antiviral immunity and beyond. *Nat. Rev. Microbiol.* 16: 423–439.
- Malakhov, M. P., O. A. Malakhova, K. I. Kim, K. J. Ritchie, and D. E. Zhang. 2002. UBP43 (USP18) specifically removes ISG15 from conjugated proteins. *J. Biol. Chem.* 277: 9976–9981.
- Zhang, X., D. Bogunovic, B. Payelle-Brogard, V. Francois-Newton, S. D. Speer, C. Yuan, S. Volpi, Z. Li, O. Sanal, D. Mansouri, et al. 2015. Human intracellular ISG15 prevents interferon- $\alpha/\beta$  over-amplification and auto-inflammation. *Nature* 517: 89–93.
- François-Newton, V., G. Magno de Freitas Almeida, B. Payelle-Brogard, D. Monneron, L. Pichard-Garcia, J. Pehler, S. Pellegrini, and G. Uzé. 2011. USP18-based negative feedback control is induced by type I and type III interferons and specifically inactivates interferon  $\alpha$  response. *PLoS One* 6: e22200.
- Malakhova, O. A., K. I. Kim, J. K. Luo, W. Zou, K. G. Kumar, S. Y. Fuchs, K. Shuai, and D. E. Zhang. 2006. UBP43 is a novel regulator of interferon signaling independent of its ISG15 isopeptidase activity. *EMBO J.* 25: 2358–2367.
- Sarasin-Filipowicz, M., X. Wang, M. Yan, F. H. Duong, V. Poli, D. J. Hilton, D. E. Zhang, and M. H. Heim. 2009. Alpha interferon induces long-lasting refractoriness of JAK-STAT signaling in the mouse liver through induction of USP18/UBP43. *Mol. Cell. Biol.* 29: 4841–4851.
- Speer, S. D., Z. Li, S. Buta, B. Payelle-Brogard, L. Qian, F. Vigant, E. Rubino, T. J. Gardner, T. Wedeking, M. Hermann, et al. 2016. ISG15 deficiency and increased viral resistance in humans but not mice. *Nat. Commun.* 7: 11496.
- Vuillier, F., Z. Li, P. H. Commere, L. T. Dynesen, and S. Pellegrini. 2019. USP18 and ISG15 coordinately impact on SKP2 and cell cycle progression. *Sci. Rep.* 9: 4066.
- Hermann, M., and D. Bogunovic. 2017. ISG15: in sickness and in health. *Trends Immunol.* 38: 79–93.
- Andrejeva, J., H. Norsted, M. Habjan, V. Thiel, S. Goodbourn, and R. E. Randall. 2013. ISG56/IFIT1 is primarily responsible for interferon-induced changes to patterns of parainfluenza virus type 5 transcription and protein synthesis. *J. Gen. Virol.* 94: 59–68.
- Domingues, P., C. G. Bamford, C. Boutell, and J. McLauchlan. 2015. Inhibition of hepatitis C virus RNA replication by ISG15 does not require its conjugation to protein substrates by the HERC5 E3 ligase. *J. Gen. Virol.* 96: 3236–3242.
- Sanjana, N. E., O. Shalem, and F. Zhang. 2014. Improved vectors and genome-wide libraries for CRISPR screening. *Nat. Methods* 11: 783–784.
- Durbin, A. P., J. M. McAuliffe, P. L. Collins, and B. R. Murphy. 1999. Mutations in the C, D, and V open reading frames of human parainfluenza virus type 3 attenuate replication in rodents and primates. *Virology* 261: 319–330.
- Hilton, L., K. Moganeradj, G. Zhang, Y. H. Chen, R. E. Randall, J. W. McCauley, and S. Goodbourn. 2006. The NPro product of bovine viral diarrhoea virus inhibits

- DNA binding by interferon regulatory factor 3 and targets it for proteasomal degradation. *J. Virol.* 80: 11723–11732.
22. Choppin, P. W. 1964. Multiplication of a myxovirus (Sv5) with minimal cytopathic effects and without interference. *Virology* 23: 224–233.
  23. Didcock, L., D. F. Young, S. Goodbourn, and R. E. Randall. 1999. The V protein of simian virus 5 inhibits interferon signalling by targeting STAT1 for proteasome-mediated degradation. *J. Virol.* 73: 9928–9933.
  24. Randall, R. E., D. F. Young, K. K. Goswami, and W. C. Russell. 1987. Isolation and characterization of monoclonal antibodies to simian virus 5 and their use in revealing antigenic differences between human, canine and simian isolates. *J. Gen. Virol.* 68: 2769–2780.
  25. Rydbeck, R., C. Orvell, A. Löve, and E. Norrby. 1986. Characterization of four parainfluenza virus type 3 proteins by use of monoclonal antibodies. *J. Gen. Virol.* 67: 1531–1542.
  26. Wignall-Fleming, E. B., D. J. Hughes, S. Vattipally, S. Modha, S. Goodbourn, A. J. Davison, and R. E. Randall. 2019. Analysis of paramyxovirus transcription and replication by high-throughput sequencing. *J. Virol.* DOI: 10.1128/JVI.00571-19.
  27. Young, D. F., J. Andrejeva, X. Li, F. Inesta-Vaquera, C. Dong, V. H. Cowling, S. Goodbourn, and R. E. Randall. 2016. Human IFIT1 inhibits mRNA translation of rubulaviruses but not other members of the paramyxoviridae family. *J. Virol.* 90: 9446–9456.
  28. Killip, M. J., D. F. Young, C. S. Ross, S. Chen, S. Goodbourn, and R. E. Randall. 2011. Failure to activate the IFN- $\beta$  promoter by a paramyxovirus lacking an interferon antagonist. *Virology* 415: 39–46.
  29. Killip, M. J., D. F. Young, D. Gatherer, C. S. Ross, J. A. Short, A. J. Davison, S. Goodbourn, and R. E. Randall. 2013. Deep sequencing analysis of defective genomes of parainfluenza virus 5 and their role in interferon induction. *J. Virol.* 87: 4798–4807.
  30. Chen, C., R. W. Compans, and P. W. Choppin. 1971. Parainfluenza virus surface projections: glycoproteins with haemagglutinin and neuraminidase activities. *J. Gen. Virol.* 11: 53–58.
  31. Young, D. F., E. B. Wignall-Fleming, D. C. Busse, M. J. Pickin, J. Hankinson, E. M. Randall, A. Tavendale, A. J. Davison, D. Lamont, J. S. Tregoning, et al. 2019. The switch between acute and persistent paramyxovirus infection caused by single amino acid substitutions in the RNA polymerase P subunit. *PLoS Pathog.* 15: e1007561.
  32. Bogunovic, D., M. Byun, L. A. Durfee, A. Abhyankar, O. Sanal, D. Mansouri, S. Salem, I. Radovanovic, A. V. Grant, P. Adimi, et al. 2012. Mycobacterial disease and impaired IFN- $\gamma$  immunity in humans with inherited ISG15 deficiency. *Science* 337: 1684–1688.
  33. Diab, M., A. Vitenshtein, Y. Drori, R. Yamin, O. Danziger, R. Zamostiano, M. Mandelboim, E. Bacharach, and O. Mandelboim. 2016. Suppression of human metapneumovirus (HMPV) infection by the innate sensing gene CEACAM1. *Oncotarget* 7: 66468–66479.
  34. Vitenshtein, A., Y. Weisblum, S. Hauka, A. Halenius, E. Oiknine-Djian, P. Tsukerman, Y. Bauman, Y. Bar-On, N. Stern-Ginossar, J. Enk, et al. 2016. CEACAM1-mediated inhibition of virus production. *Cell Rep.* 15: 2331–2339.
  35. Muenzner, P., M. Naumann, T. F. Meyer, and S. D. Gray-Owen. 2001. Pathogenic *Neisseria* trigger expression of their carcinoembryonic antigen-related cellular adhesion molecule 1 (CEACAM1; previously CD66a) receptor on primary endothelial cells by activating the immediate early response transcription factor, nuclear factor-kappaB. *J. Biol. Chem.* 276: 24331–24340.
  36. Gray-Owen, S. D., and R. S. Blumberg. 2006. CEACAM1: contact-dependent control of immunity. *Nat. Rev. Immunol.* 6: 433–446.
  37. Michalska, A., K. Blaszczyk, J. Wesoly, and H. A. R. Bluyssen. 2018. A positive feedback amplifier circuit that regulates interferon (IFN)-stimulated gene expression and controls type I and type II IFN responses. *Front. Immunol.* 9: 1135.
  38. Polymenis, M., and R. Aramayo. 2015. Translate to divide: control of the cell cycle by protein synthesis. *Microb. Cell* 2: 94–104.
  39. Stumpf, C. R., M. V. Moreno, A. B. Olshen, B. S. Taylor, and D. Ruggero. 2013. The translational landscape of the mammalian cell cycle. *Mol. Cell* 52: 574–582.